



This is a repository copy of *The effect of high-temperature creep on buckling behaviour of aluminium grade EN6082AW T6 columns*.

White Rose Research Online URL for this paper:
<http://eprints.whiterose.ac.uk/157408/>

Version: Accepted Version

Article:

Torić, N., Boko, I., Burgess, I.W. orcid.org/0000-0001-9348-2915 et al. (1 more author) (2020) The effect of high-temperature creep on buckling behaviour of aluminium grade EN6082AW T6 columns. *Fire Safety Journal*, 112. ISSN 0379-7112

<https://doi.org/10.1016/j.firesaf.2020.102971>

Article available under the terms of the CC-BY-NC-ND licence
(<https://creativecommons.org/licenses/by-nc-nd/4.0/>).

Reuse

This article is distributed under the terms of the Creative Commons Attribution-NonCommercial-NoDerivs (CC BY-NC-ND) licence. This licence only allows you to download this work and share it with others as long as you credit the authors, but you can't change the article in any way or use it commercially. More information and the full terms of the licence here: <https://creativecommons.org/licenses/>

Takedown

If you consider content in White Rose Research Online to be in breach of UK law, please notify us by emailing eprints@whiterose.ac.uk including the URL of the record and the reason for the withdrawal request.



eprints@whiterose.ac.uk
<https://eprints.whiterose.ac.uk/>

THE EFFECT OF HIGH-TEMPERATURE CREEP ON BUCKLING BEHAVIOUR OF ALUMINIUM GRADE EN6082AW T6 COLUMNS

Neno Torić^{1*}, Ivica Boko¹, Ian W. Burgess² and Vladimir Divić¹

Abstract:

The paper presents an experimental study that investigates the influence of high-temperature creep on reduction of the buckling load capacity of aluminium grade EN6082AW T6 columns. The study was performed by performing constant-temperature capacity and creep tests on 17 column specimens of approximately 2.6 m length. A total of eight capacity tests and nine creep tests were carried out. Results obtained within the study have revealed a critical temperature interval of 160-260°C within which high-temperature creep significantly influences the columns' buckling load capacity. The load level at which high-temperature creep influences the reduction of columns' buckling-load capacity, by exhibiting low short-term creep resistance, is above 90% of the column's axial load capacity. The occurrence of short-term creep resistance is present within the whole temperature interval of 160-260°C. The study provides relevant thermo-mechanical criteria for the assessment of creep-induced buckling of the tested aluminium alloy.

Keywords:

Aluminium, fire, columns, creep, EN6082AW T6, stress

—

¹ University of Split, Faculty of Civil Engineering, Architecture and Geodesy, Matice Hrvatske 15, 21000 Split, Croatia, Tel: +385-21-303-366, Fax: +385-21-303-331

* E-mail: neno.toric@gradst.hr (corresponding author)

² University of Sheffield, Department of Civil and Structural Engineering, Sir Frederick Mappin Building, Mappin Street, Sheffield, S1 3JD, UK.

1. INTRODUCTION

1.1 *Motivation*

Aluminium structures have slowly begun to take their place in modern engineering practice, as a suitable choice of material for building structures [1]. The reasons for applying aluminium in construction practice can be briefly summarized as follows. Positive attributes such as one third of the self-weight of traditional steel structures, together with comparable strength, are very much in line with the demands of current construction practice. As an example, modern structural aluminium alloys, such as the 6xxx series, have proof strengths at ambient temperature equivalent to those of steel grades S235, S275 and S355. The alloy 6082AW T6 that is investigated in this paper has a proof strength with a minimum value of 260 MPa. The main disadvantage to the application of aluminium in construction practice is that it is more susceptible to the effects of normal building fire temperatures. As well as faster heating due to its higher value of thermal conductivity, and its rapid strength reduction within the temperature interval 200-350°C, aluminium is more susceptible to the development of creep at high temperatures, which is related to its lower melting temperature than steel. Aluminium alloys tend to have melting temperatures in the range 550-600°C [2]. Therefore, creep strain in aluminium tends to develop at lower temperatures than in steel, and consequently has a higher influence on the behaviour in fire of aluminium structures [2]. According to a recent coupon study conducted on alloy 6082AW T6 [3], the critical temperature for the onset of creep development is approximately 200°C, which is about half the comparable value in the case of steel [4]. This indicates that high-temperature creep might induce earlier failure in aluminium members, whether they are predominantly loaded in compression or in bending. Since detailed experimental data on the creep behaviour of aluminium alloy 6082AW T6 is relatively scarce, a three-year collaborative research project [3-5] between Universities of Split and Sheffield was initiated. One of this project's objectives was to investigate the effect of high-temperature creep on the reduction of the fire resistance of aluminium columns; in particular the effect of load ratio on the reduction of fire resistance under prolonged exposure to high-temperature. One of the project's scientific interests was to

quantify the inherent fire resistance period of aluminium columns with prolonged fire exposure, and to investigate the critical temperature interval within which creep might cause premature buckling failure. These parameters are essential for understanding the level of impact of creep on the column behaviour during prolonged fire exposure. This needs to be investigated in order to aid the development of performance-based design methods which model the different fire time-temperature curves that are possible in realistic fires. A large spectrum of heating rates is possible in real fire situations, including situations in which fires have low heating rates but long duration. The most common context for slow heating is in fire-protected members or members that are relatively remote from a localised fire source.

1.2 Previous research

High-temperature test studies of aluminium columns are very rare among published research on the behaviour of aluminium in fire. Studies by Langhelle [6] and Eberg *et al.* [7] analysed the buckling behaviour of aluminium columns (of alloys 6082-T4 and 6082-T6) exposed to high temperatures. The objective of these studies was the experimental validation and calibration of nonlinear finite element models for use in the design of fire-exposed aluminium structures. Both constant- and transient-temperature tests were conducted in these studies. Amongst other findings, it was observed that the load-bearing capacities calculated using the Eurocode 9 [8] methodology were conservative for both high-temperature test types.

Further research on the behaviour of aluminium structures in fire was conducted by Maljaars [9] on alloys 5083-H111 and 6060-T66. This study focused on the analysis of local buckling of aluminium sections, in which short aluminium members were exposed to axial compressive force at high temperatures. The results showed that high-temperature creep reduces the aluminium's compressive strength in transient testing, which represents a fairly realistic representation of the temperature increase of structural members in building fires. The same authors proposed [10] new material creep parameters suitable for the aluminium alloys tested, and these were validated using Harmathy's creep model [11].

The high-temperature behaviour of aluminium beams (alloys 5083-H112 and 6060-T66) has recently been investigated by Zheng and Zhang [12]. Practical formulas for calculating the temperature increase in unprotected and protected aluminium beams were proposed, suggesting that the critical temperature approach of Eurocode 9 provides conservative predictions of load bearing capacity. Jiang *et al.* [13] conducted a comprehensive study on the buckling performance of aluminium (6061-T6 alloy) columns under constant temperatures up to 400°C. As a result of the study, stability coefficients were calculated and compared to the existing code-based values. The importance of taking creep into account in general structural behaviour is also evident when considering the behaviour of connections in fire conditions, as suggested in recent numerical study by Hantouche *et al.* [14].

Apart from the research mentioned above, only a handful of publications can be found on the subject of the development of creep models for aluminium at high temperatures and the influence of creep on the load-bearing capacity of aluminium structures, particularly columns. Since the critical temperature interval for creep development coincides with the critical temperature interval over which the strength of the aluminium is reduced, it is necessary to quantify the effect that creep has on column specimens of a realistic scale within this overlapping temperature interval.

2. EXPERIMENTAL STUDY

2.1 Test setup and methodology

Column testing within the project was carried out in the structural laboratory of the Faculty of Civil Engineering, Architecture and Geodesy at the University of Split. A reaction frame structure composed of UPN280 steel sections was used as the stiff frame for external load application on the columns. A schematic diagram of the entire test setup is presented in Figure 1.

Because of the limitations of the reaction frame structure, the maximum tested length of the column specimens was approximately 2.6 m. The slenderness ratio of all the aluminium columns tested (I section with dimensions 220/170/15/9) was approximately 70. The load on the column was applied axially using a hydraulic ram (max. 1500 kN)

supported by the reaction frame. A small lateral load, used to simulate geometrical imperfections and to reduce the friction at the column supports, was applied by hydraulic rams (max. 300 kN). This lateral load was applied about the column's weak axis, in order to induce the principal buckling mode in the plane of the stiff frame. The pressure inside the rams was monitored and controlled according to the experiment protocol, using digital pressure gauges. Lateral displacements of the columns were recorded using LVDT transducers. Two transducers were located on the column; one at the centre of the cross-section in the transverse direction and other in the axial direction at the column end. Heating of the column utilized induction heaters, which are considered to be superior to electrical resistance elements, in terms of uniformity of heating. The main advantage of induction heating was the possibility of very uniform heating of complex cross-sections without the need to construct a large furnace around the test specimen. The induction heating method is a safer approach, since the induction heater does not increase its own temperature and therefore reduce the specimen's emissivity values due to burning isolation and ceramic elements during a test. Induction heating is also more energy-efficient, with better heat transfer between the induction heater and the test specimen. An indirect method was used for heating of the aluminium columns. This was necessary since aluminium does not possess ferromagnetic properties that would allow heating of the column by induced eddy-currents. This indirect heating was achieved by induction heating of a 12mm thick cylindrical steel jacket with an outer diameter of 406 mm surrounding the heated part of the column. In order to reduce heat loss and to protect the surrounding equipment, the steel tube was thermally insulated outside with ceramic wool which provided thermal resistance up to 800°C. The cables directly heated the steel jacket, at heating rates ranging between 2°C and 10°C/min, depending on the output power of the induction source. The heating rate was controlled by an additional thermocouple attached to the inner surface of the jacket at mid-span. Temperatures were measured using thermocouples located at several points along the column length (Figure 2). A plot of the temperature variation during the creep tests at 160°C, 220°C and 260°C are presented in Figure 3.

The data recorded from the pressure gauge in the hydraulic rams, the displacement transducers and the thermocouples were transferred to a central data-acquisition card, and subsequently stored on a PC. The testing methodology for the aluminium columns in this

research relies on the stationary testing method, in which the columns are heated to a predetermined temperature, which is then held constant, and subsequently loaded up to failure. The temperature ranges for the stationary tests were within the temperature interval 160-260°C, with the load levels varying over a range of load ratios at the target temperature.

Steel pins with 60 mm diameter were used as simple supports at the ends of the columns. The pins were used together with a thin steel plate which was lubricated on both surfaces in order to reduce the friction occurring in this area. A total of 17 columns were tested within the study; 8 for constant-temperature capacity tests and 9 for constant-temperature creep tests.

2.2 Constant-temperature capacity tests

The purpose of these tests was to find the axial load (buckling) capacity of the column at target temperature levels. They were conducted by applying a constant transverse force and subsequently axial force at a rate of 10 kN/s, up to the point at which global buckling occurs. The value of the transverse force at each temperature level was subsequently reduced in proportion to the reduction factors for modulus of elasticity obtained from a previous coupon study [3], which was based on specimens obtained directly from column flanges.

The results of the capacity tests are given in Figure 4, for target temperatures of 20, 160, 220 and 260°C. A comparison is also shown against the predictions of the research software *Vulcan* utilizing rotational springs as is discussed in sub-chapter 3.1. The simulations presented in Figure 4 utilized the material stress-strain model obtained [3] from the previous coupon study. A summary of the test parameters for the column capacity tests which are used in the numerical analysis are presented in Table 1. Two capacity tests were conducted at each temperature level in order to obtain a more reliable estimate of the column's buckling capacity.

2.3 Constant-temperature creep tests

These tests were conducted by gradual heating of the column to a target temperature, followed by loading it to a constant value of transverse force. Then a constant axial force is applied to the column and maintained until global buckling of the column due to creep occurs. The load ratios applied during the creep tests are represented as the applied axial load as a fraction of the axial load capacity at the target temperature obtained from the tests described in sub-chapter 2.2; this can be represented by the expression:

$$\varphi = \frac{F_{b,\theta}}{F_{cap,\theta}} \quad (1)$$

in which $F_{b,\theta}$ is the applied compressive force during a creep test at temperature θ and $F_{cap,\theta}$ is its buckling capacity at temperature level θ .

Within the duration of a creep test, both external loads, as well as the target temperature of the column, are maintained (Figure 3). The target temperatures of the creep tests were chosen to match the target temperatures of the capacity tests conducted previously. A summary of the test parameters for the column creep tests is presented in Table 2. Three creep tests, at temperatures 160-220-260°C, were conducted, in order to explore the effect of creep in reducing the column's buckling capacity.

2.4 Test failure criteria

The failure criterion for the capacity and creep tests conducted is based on the reduced level of the axial force at the onset of column buckling. This criterion is based on a 10% reduction of axial force after the loss of column stiffness due to global buckling, beyond which the experiment is terminated. This force reduction is usually followed by the occurrence of vertical asymptote in the time-dependent plot of column's axial displacement.

3. MODELLING OF THE TESTS

3.1 Numerical model

The academic version of *Vulcan* [15, 16] used for modelling the tests is based on geometrically nonlinear structural analysis. The temperature of a member within the software can be inserted directly into the input file by specifying the temperature of the upper and lower flanges, and the section's web. For modelling of the column tests three-noded beam elements from the *Vulcan* finite element database have been used. A total of 26 three-node line elements are applied as a linear mesh with an I-section segmentation matrix of 13x11, which allows temperatures and material properties to vary across the section. The model is shown in Figure 5(a). The numerical modelling presented in this section relies on the material test data obtained from the previous research study [3]. The material test data used in the numerical model is based on a coupon study of specimens cut from column flanges. This coupon study provides information on the proof strength (stress at 0.2% strain) of the aluminium, its ultimate strength, stress-strain curves and modulus of elasticity at temperatures up to 350°C. The temperature-dependent degradation of proof stress and modulus are shown in Figure 5(b). An explicit creep model is utilized from the coupon study mentioned, and this has been programmed into the *Vulcan* software in order to model the development of creep strain in the column creep tests. Temperature measurements taken during the tests were directly used as input data for the model.

3.2 Material modelling

Total strain in fire-exposed metallic structures is composed of three components [17]:

$$\varepsilon_{\text{tot}} = \varepsilon_{\text{th}}(T) + \varepsilon_{\sigma}(\sigma, T) + \varepsilon_{\text{cr}}(\sigma, T, t) \quad (2)$$

where : $\varepsilon_{\text{th}}(T)$ is the temperature-dependent thermal strain, $\varepsilon_{\sigma}(\sigma, T)$ is the stress-related (mechanical) strain, and $\varepsilon_{\text{cr}}(\sigma, T, t)$ is the stress-, temperature- and time-dependent creep strain. By separating the three strain components, as suggested by Anderberg [17], it is possible to include creep explicitly into structural fire analysis.

The (mechanical) stress-strain model for the tested aluminium is based on a Ramberg-Osgood law [8, 18]:

$$\varepsilon_{\sigma} = \frac{\sigma}{E_{y,\theta}} + 0.002 \cdot \left(\frac{\sigma}{f_{0.2,\theta}} \right)^n \quad (3)$$

in which

$$n = \frac{\ln(0.002 / \varepsilon_{u,\theta})}{\ln(f_{0.2,\theta} / f_{u,\theta})} \quad (4)$$

where n represents the degree of hardening of the curve, $E_{y,\theta}$ is the modulus of elasticity at temperature θ , $f_{0.2,\theta}$ is the stress at 0.2% strain and temperature θ , $f_{u,\theta}$ is the ultimate strength at temperature θ , and $\varepsilon_{u,\theta}$ is the strain value at $f_{u,\theta}$. The values of the coefficient n , the proof stress $f_{0.2,\theta}$ and modulus $E_{y,\theta}$ are taken from [3] and are presented in Tables 4 and 5. Figure 5(c) presents a plot of the stress-strain curves given by the stress-strain model from Equations (2)-(3).

As stated previously, a creep model derived from study [3] was also implemented in the *Vulcan* software. The creep model is valid within the temperature range 200-300°C. The model is based on a double- curvature curve:

$$\varepsilon_{cr}(\sigma, T, t) = c + a \cdot t^b + e \cdot t^f \quad (5)$$

in which ε_{cr} - creep strain (%), t is time (min) and $c = \frac{\sigma}{E_{y,\theta}}$ is elastic strain. Coefficients a ,

b , e and f are documented in reference [3]. Elastic strain is implicitly calculated by *Vulcan*, and therefore the value of elastic strain is removed from the creep equation.

3.3 The friction model

The friction in the pin-supports cannot be neglected, and an appropriate numerical model needs to take this effect into account. The influence of friction on the behaviour of restrained and unrestrained steel columns has been reported by Tan *et al.* [19] and by Torić *et al.* [20]. In order to take into account the inherent friction a suitable rotational spring with constant stiffness is inserted at each support, in similar fashion to the approach adopted in [19].

An optimization strategy to select a stiffness value was performed in order to closely match the axial failure loads of columns in the capacity tests. For a given value of transverse force, axial load is incrementally increased up to the occurrence of column buckling failure. If necessary the spring stiffness is then increased by 10% in order to increase the buckling force. This is performed up to the point at which the buckling force obtained from the model is closest to the experimental one. As a result, a temperature- dependent stiffness value can be obtained. The values of the rotational stiffness constant at each temperature level are presented in Table 3. The predictions of the numerical model with rotational springs are also given in the same table. The same stiffness coefficients are used for modelling of the subsequent stationary creep tests performed at 220°C and 260°C. A comparison between the buckling capacities obtained from the *Vulcan* model and the capacity tests at 220°C and 260°C is also presented in Table 3.

3.4 Failure criteria of the numerical model

The failure criterion of the numerical model is based on the loss of convergence for the column's displacement during the quasi-static analysis. The convergence criterion in the *Vulcan* software is based on a prescribed displacement tolerance between subsequent displacement field calculations which is set to the value 1.00E-04.

3.5 Presentation of the test results

The comparison between the axial displacements obtained from explicit creep modelling using the *Vulcan* software and the conducted creep tests is presented in Figures 6 and 7. The tested column specimens are presented in Figure 8; Figure 8(a) shows creep-test specimens and Figure 8(b) shows capacity-test specimens. In the case of creep tests, four specimens had a symmetric buckling shape while five specimens were slightly asymmetric, with the location of the plastic hinge being displaced by between 2 and 20 cm from the mid-span of the specimen. In the case of capacity tests, four out of the eight specimens had a symmetrical buckling shape, while the rest had unsymmetrical buckling shapes similar to those generated in the creep tests. This might be attributed to the fact that the transverse ram was not located exactly at the mid-span of the column, as can be seen in the column model shown in Figure 5(a). Figure 9 shows the accuracy of the applied

numerical model in modelling the capacity tests (Figure 9a) and the creep tests (Figure 9b); the $\pm 10\%$ margin lines are also shown.

4. DISCUSSION OF RESULTS

4.1 Prediction of column failure times and the capacities

It can be seen from Figure 9(a) for the axial load capacity tests, that all results obtained by the numerical model correlate well with the experimental results, lying within the $\pm 10\%$ error margin. This illustrates that the modelling approach of using rotational springs to represent hinge friction is justifiable, at least for these tests. Figure 9(b) shows that the explicit creep modelling scheme utilized by Vulcan is also capable of predicting the failure times of aluminium columns with sufficient accuracy, with the modelling results falling either within the $\pm 10\%$ error margin or on the safe side. The column creep tests at 160°C were not modelled, since the analytical creep model from study [3] is only valid within the temperature range $200\text{-}300^\circ\text{C}$.

4.2 Influence of load ratio on creep development

It can be seen from the test results presented in Table 2 that high-temperature creep can induce column failure at temperatures starting from 160°C when the column is exposed to high load-levels (greater than or equal to 88% of the columns' axial load capacity at the target temperature level). The influence of creep is also present at lower load-levels as temperatures increase, as can be seen from Figures 6 and 7. The short-term creep resistance of 6082 T6 columns can be considered to be rather low at load levels above 85% of the columns' axial load capacity and within the temperature region $160\text{-}260^\circ\text{C}$, as can be seen from the results presented in Table 2. These observations are similar to those concerning the short-term creep resistance of steel grade S275 columns from a previous study [20], in which short-term creep resistance was also reported as low for load levels above 90% of the columns' axial load capacity and within the temperature interval $400\text{-}600^\circ\text{C}$. This indicates that suitable safety factors might generally be necessary against the occurrence of time-dependent deformations in all metallic structures exposed to prolonged fire

exposure. However, this needs to be investigated further in future column studies. It should be noted that the lowest load level used in the current study was 77% at 260°C, emphasising that the study was focused on load levels relatively close to the columns' buckling capacity for short-term temperature exposure, the objective being to test columns' creep performance under realistic load conditions.

4.3 Creep buckling time

All nine column creep tests exhibited failure within the 240-minute interval which represents the generally relevant fire resistance period of building structures. Looking at the failure times of the aluminium columns shown in Table 2, it is apparent that the failure times were relatively short for load ratios above approximately 85% within the temperature interval 160-260°C. This is in line with the codified design procedure given in EN1999-1-2 [21], which mandates the use of a constant safety factor of 1.2 on the design buckling resistance of aluminium columns in fire in order to take into account the effect of high-temperature creep in reducing buckling capacity.

4.4 The effect of friction at hinged supports

The friction effect was most pronounced when testing columns at the higher temperature levels, as is apparent from Table 3. This can be observed in the increase of the rotational spring coefficient which is necessary when modelling the capacity tests at 220°C and 260°C compared with the tests at 20°C and 160°C, when the authors used the approach described in Section 2.1 to tackle the support friction problem.

4.5 Material modelling

It should be noted that all the necessary material parameters for modelling of the column tests conducted were test-based. The material properties, such as proof stress, ultimate strength, modulus of elasticity and stress-strain curves at temperature levels up to 350°C, were used for modelling of the tests. This includes the explicit creep model for alloy 6082 T6 which is valid within the temperature range 200-300°C. It can be seen from Figure 9(b) that the explicit creep model can replicate, with sufficient accuracy, the

columns' failure times at temperatures 220°C and 260°C. The failure times predicted by the explicit creep model are all either within the $\pm 10\%$ tolerance margin or on the “safe” side, indicating that the creep model can be considered as reliable in predicting a column's failure time within this temperature range.

5. CONCLUSIONS

The results presented in the test study, together with the corresponding modelling study, point to the following conclusions:

- The buckling failure of 6082 T6 columns due to creep starts to occur at 160°C for load levels higher than 88% of the buckling load capacity at the target temperature;
- Within the tested temperature range 160-260°C and at load ratios above 85%, 6082 T6 columns exhibit low short-term creep resistance;
- The explicit creep model developed by the authors can adequately predict the columns' failure times within the test interval 220-260°C.

Acknowledgement

This work was fully supported by Croatian Science Foundation under the project *Influence of creep strain on the load capacity of steel and aluminium columns exposed to fire* (UIP-2014-09-5711). Any opinions, findings, and conclusions or recommendations expressed in this material are those of the authors and do not necessarily reflect the views of Croatian Science Foundation.

REFERENCES

- [1] Skejić, D.; Boko, I.; Torić, N. Aluminium as a modern material for structures. *Građevinar* 2015, 67, 1075–1085.

- [2] Maljaars, J.; Twilt, L.; Fellingner, J.H.H.; Snijder, H.H.; Soetens, F. “Aluminium structures exposed to fire conditions—An overview”, *Heron*; 2010, 55, 85–122.
- [3] Torić N., Brnić J., Boko I., Brčić M., Burgess I. W. and Uzelac I., “Experimental Analysis of the Behaviour of Aluminium Alloy EN6082 AW T6 at High Temperature”, *Metals*, 2017; 7:126.
- [4] Torić N., Brnić J., Boko I., Brčić M., Burgess I. W. and Uzelac Glavinić I., “Development of a High Temperature Material Model for Grade S275JR Steel”, *Journal of Constructional Steel Research*, 2017; 137:161-168.
- [5] Torić, N., Uzelac Glavinić I., Burgess, Ian W., “Development of a Rheological Model for Creep Strain Evolution in Steel and Aluminium at High Temperature“, *Fire and Materials*, 2018; 42(8):879-888.
- [6] Langhelle, N.K., Experimental validation and calibration of nonlinear finite element models for use in design of aluminium structures exposed to fire, PhD thesis, Norwegian University of Science and Technology, Trondheim, ISBN 82-471-0376-1, 1999.
- [7] Eberg, E., Amdahl, J. and Langhelle, N.K., Experimental investigation of creep behaviour of aluminium at elevated temperatures, SINTEF report no. STF22 F96713, 1996.
- [8] EN 1999-1-1:2007, *Eurocode 9 – Design of aluminium structures – Part 1-1: General structural rules*, European Committee for Standardization, Brussels, 2007.
- [9] Maljaars, J.; Soetens, F.; Snijder, H.H. “Local buckling of aluminium structures exposed to fire Part 2: Finite element models”, *Thin Walled Structures*, 2009; 47, 1418–1428.
- [10] Maljaars, J.; Soetens, F.; Katgerman, L. “Constitutive model for aluminium alloys exposed to fire conditions“, *Metall. Mater. Trans. A*, 2008; 39, 778–789.
- [11] Harmathy, T. Z., “Creep Deflections of Metal Beams in Transient Heating Processes, with Particular Reference to Fire”, *Canadian Journal of Civil Engineering*, 1976; 3, 2, 219-228.
- [12] Zheng, Y.Q. and Zhang, Z., “The fire performance and fire-resistance design of aluminium alloy I-beams“, *Fire and Materials*, 2016; 40, 141-157.
- [13] Jiang, S., Xiong, Z., Guo, X. and He, Z., “Buckling behaviour of aluminium alloy columns under fire conditions“, *Thin-Walled Structures*, 2018; 124, 523-537.
- [14] Hantouche E. G., Al Khatib, K. K., Morovat, M. A., “Modelling Creep of Steel Under Transient Temperature Conditions of Fire“, *Fire Safety Journal*, 2018; 100: 67-75.
- [15] Cai, J., Burgess, I.W. and Plank, R.J., “A generalised steel/reinforced concrete beam-column element model for fire conditions”, *Engineering Structures*, 2003; 25(6):817-833.
- [16] Sun R.-R., Huang Z., Burgess I.W., “Progressive collapse analysis of steel structures under fire conditions”, *Engineering Structures*, 2012; 34:400-413.

- [17] Anderberg, Y. “Modelling Steel Behaviour”, *Fire Safety Journal*, 1988; 13(1):17-26.
- [18] Ramberg W., Osgood W. R., Description of Stress-strain Curves by Three Parameters, Washington DC; NACA TN-902, 1943.
- [19] Tan K.-H., Toh W.-S., Huang Z.-F., Phng G.-H., “Structural Responses of Restrained Steel Columns at Elevated Temperatures Part 1: Experiments”, *Engineering Structures*, 2007; 29:1641–1652.
- [20] Torić N., Boko I., Divić V., Burgess I. W., “Behaviour of steel grade S275JR columns under the influence of high-temperature creep”, *Metals*, 2018, Vol. 8, Issue 11, paper no. 874
- [21] EN 1999-1-2:2007, *Eurocode 9 – Design of aluminium structures – Part 1-2: Structural fire design*, European Committee for Standardization, Brussels, 2007.

Figure Captions

Figure 1: Presentation of the test setup

Figure 2: Schematics of the test setup and the presentation of the temperature measuring points

Figure 3: Temperature recordings during creep tests at various temperatures

Figure 4: Column capacity tests and comparison with the applied numerical model

Figure 5: Vulcan numerical model and the applied material models

Figure 6: Results of creep tests and comparison with the numerical model – 220°C

Figure 7: Results of creep tests and comparison with the numerical model – 260°C

Figure 8: Post-test column specimens: (a) creep-test specimens (b) capacity-test specimens

Figure 9: Comparison of the predictions for column's failure time and the column's buckling capacity

Table Captions

Table 1: Test parameters for column-capacity tests

Table 2: Test parameters for column-creep tests

Table 3: Comparison between column-capacity tests and the numerical model

Table 4: Applied reduction factors for proof stress and modulus of elasticity [3]

Table 5: Applied values for the stress-strain curve factor n [3]

Nomenclature

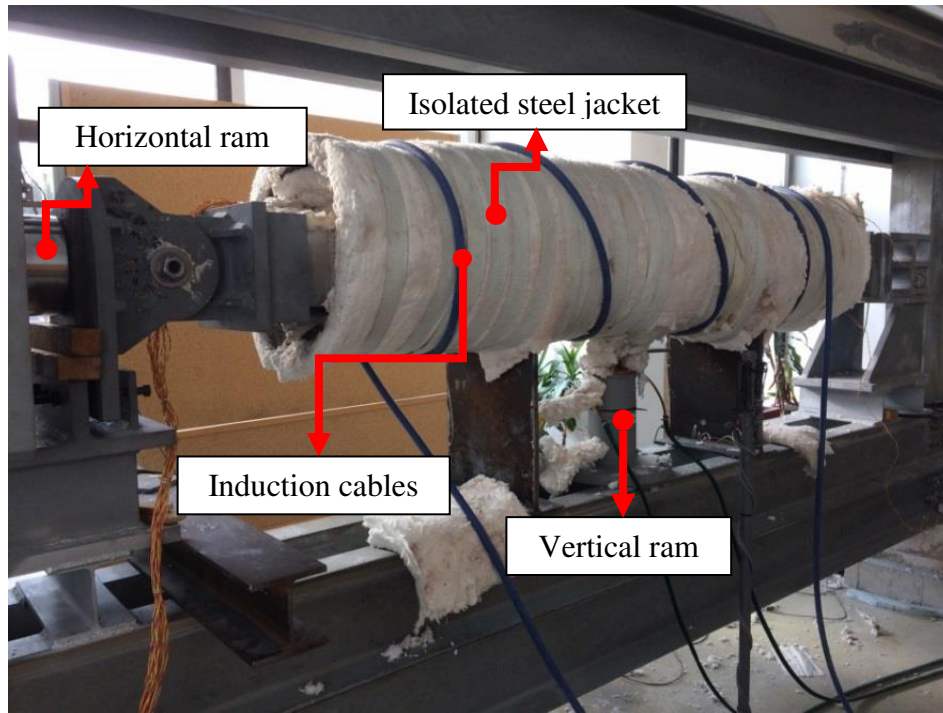
$f_{0.2,\theta}$ - stress at 0.2% strain at temperature θ

$E_{y,20}$ - modulus of elasticity at normal temperature

$E_{y,\theta}$ - modulus of elasticity at temperature θ

$k_{E\theta}$ - reduction factor for modulus of elasticity at temperature θ

$k_{0,\theta}$ - reduction factor for yield strength at temperature θ



(a) Test equipment



(b) Column specimen with thermocouples

Figure 1

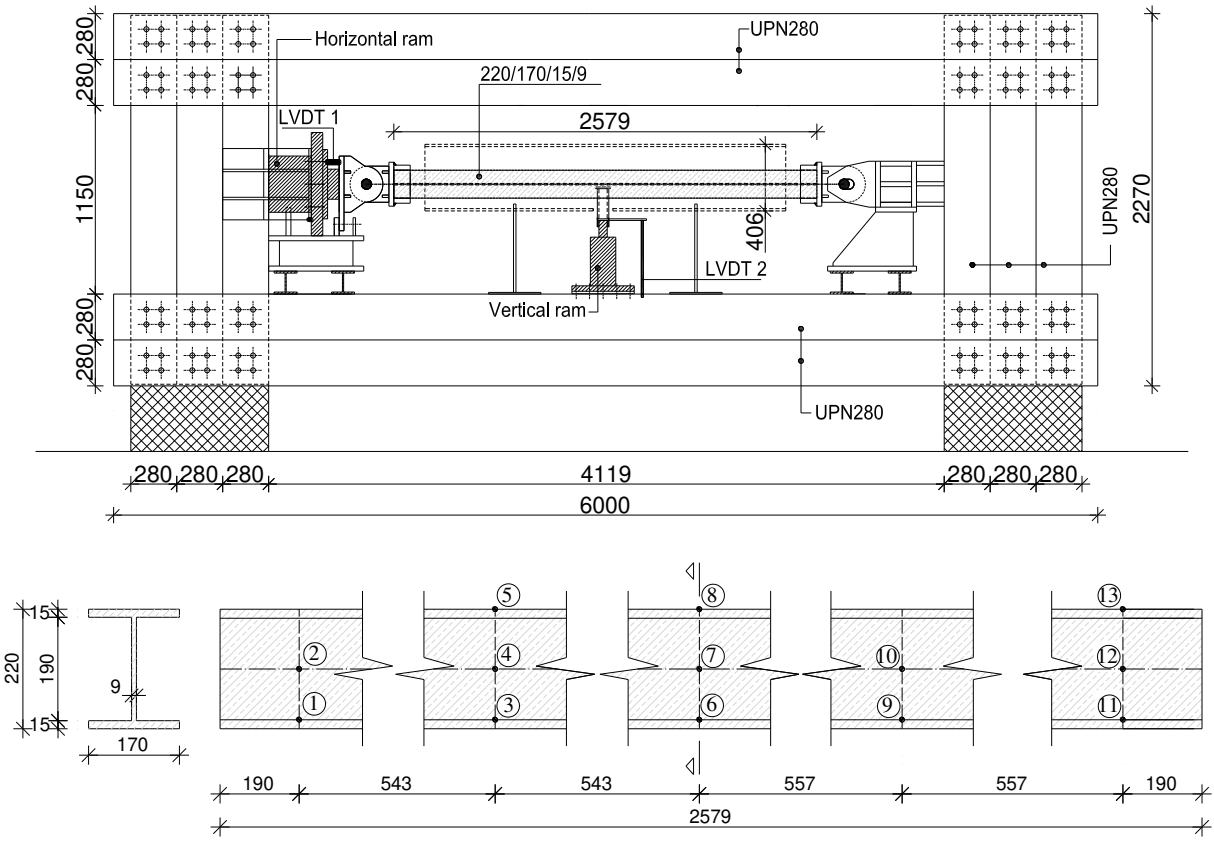
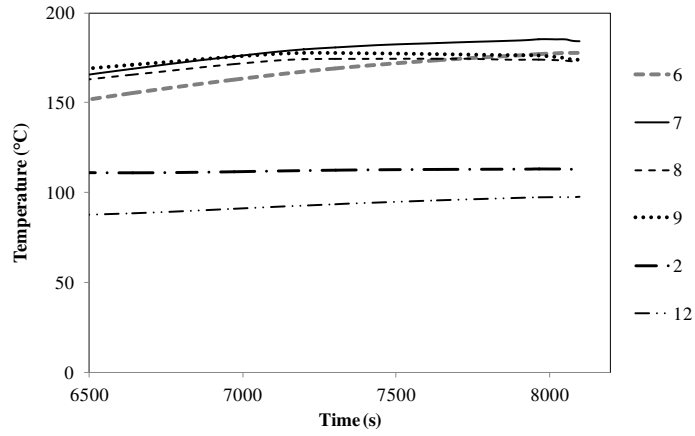
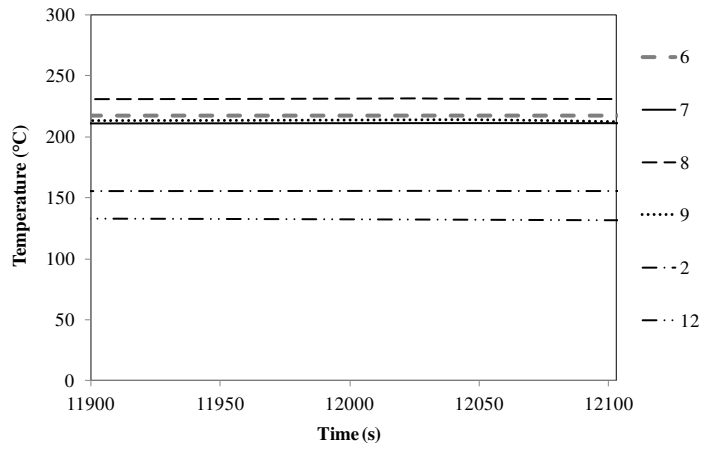


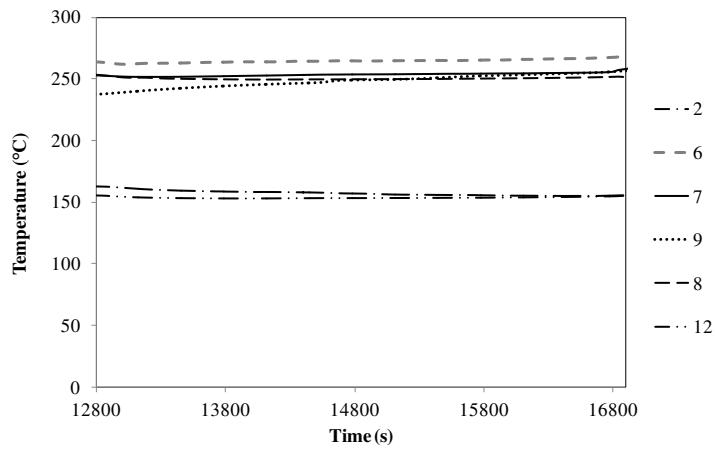
Figure 2



(a) Temperature measurements – 160°C

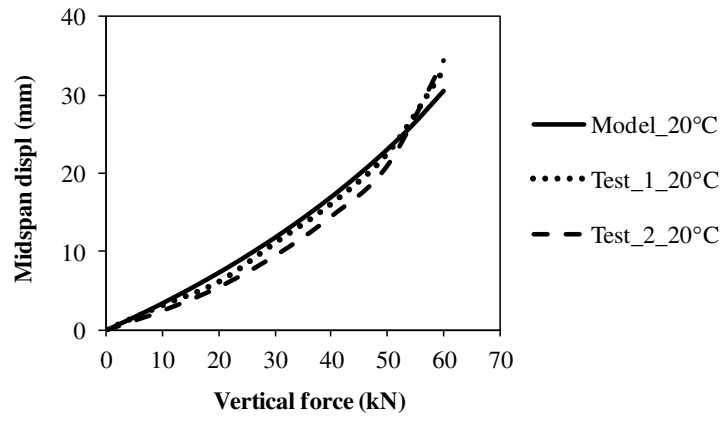


(b) Temperature measurements – 220°C

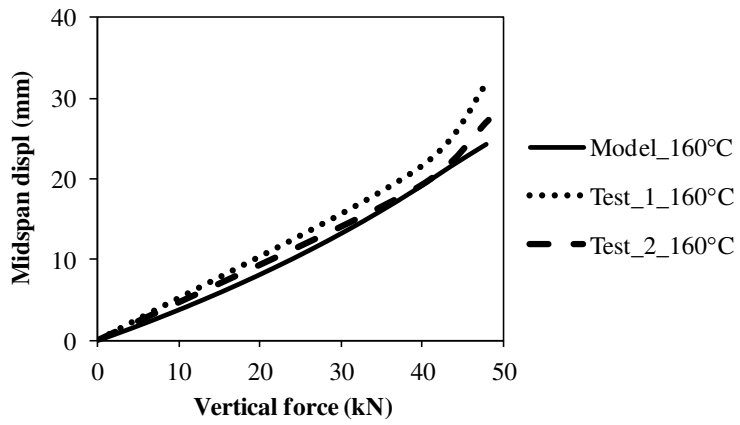


(c) Temperature measurements – 260°C

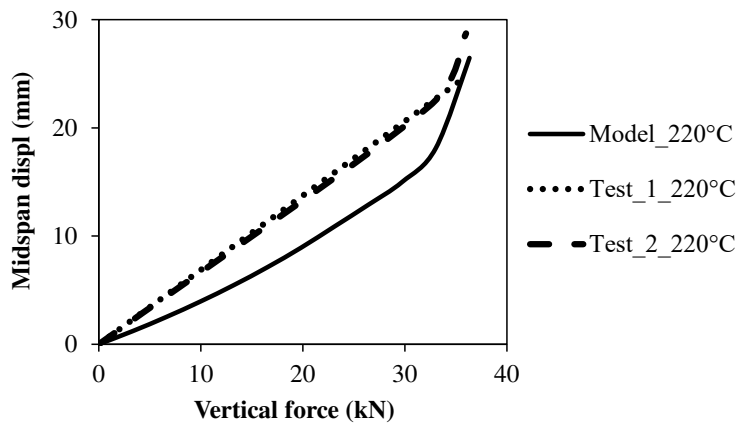
Figure 3



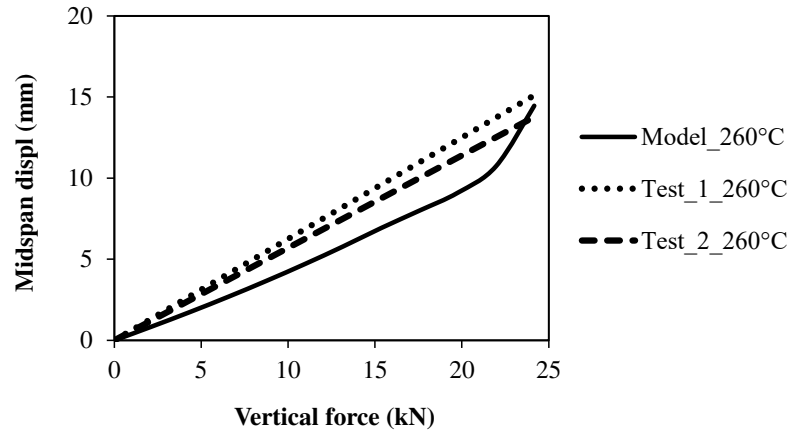
(a) 20°C



(b) 160°C

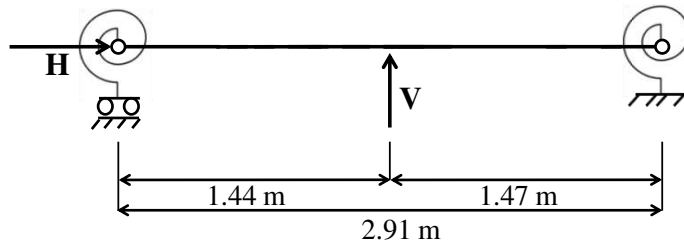


(c) 220°C

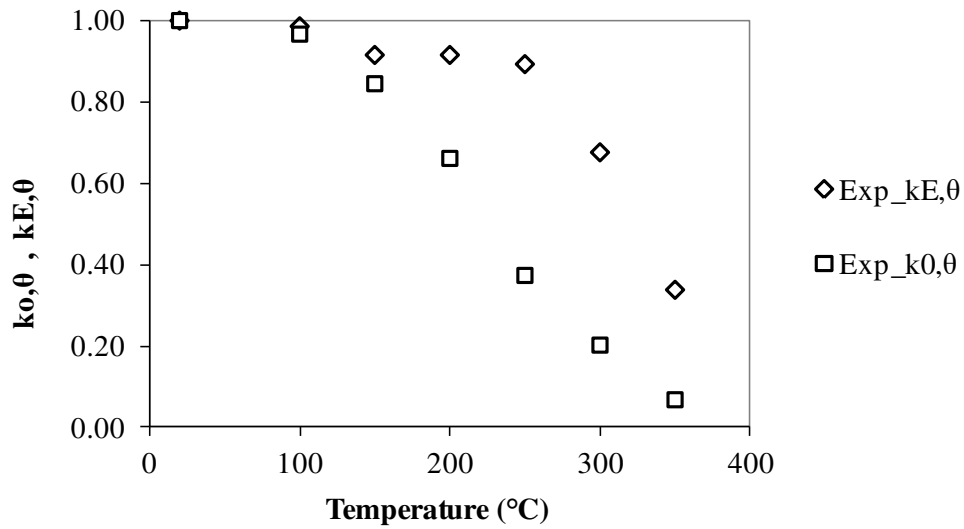


(d) 260°C

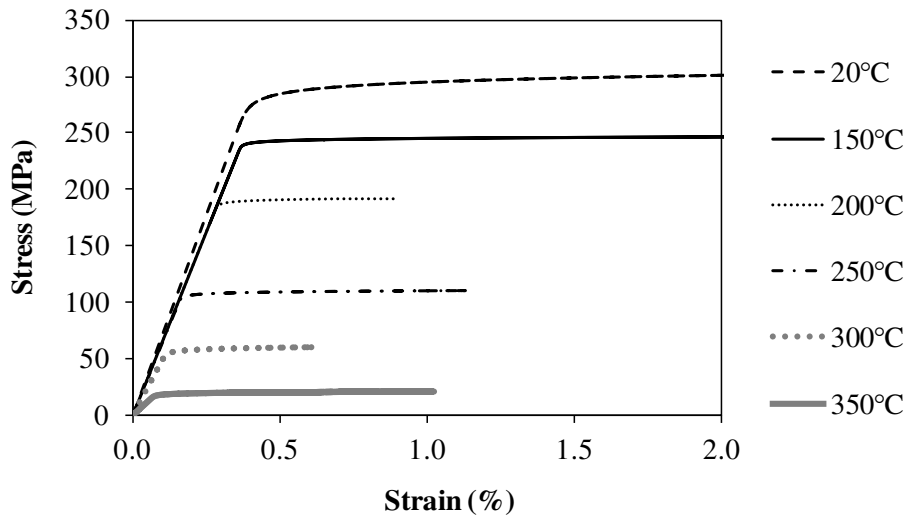
Figure 4



(a) Column model

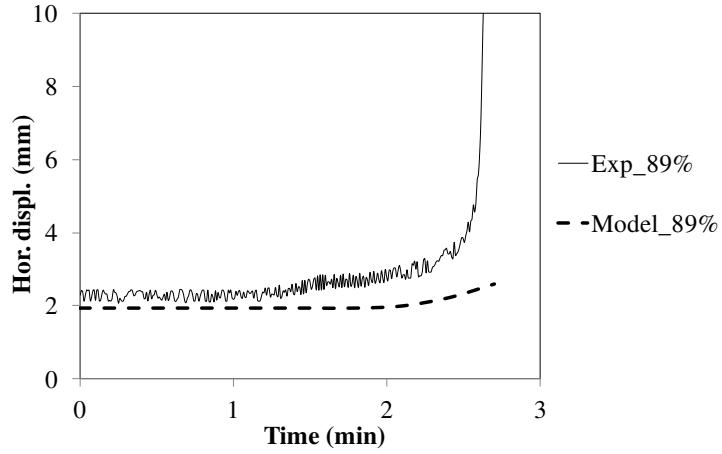


(b) Reduction factors for proof stress and modulus – 6082 T6 [3]

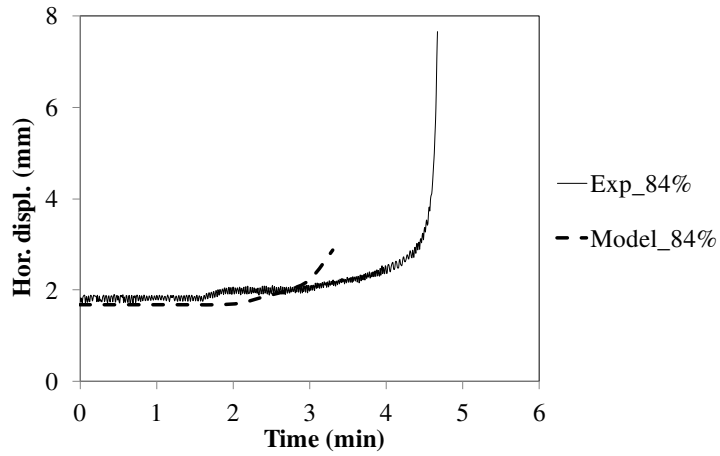


(c) Stress-strain model – 6082 T6 [3]

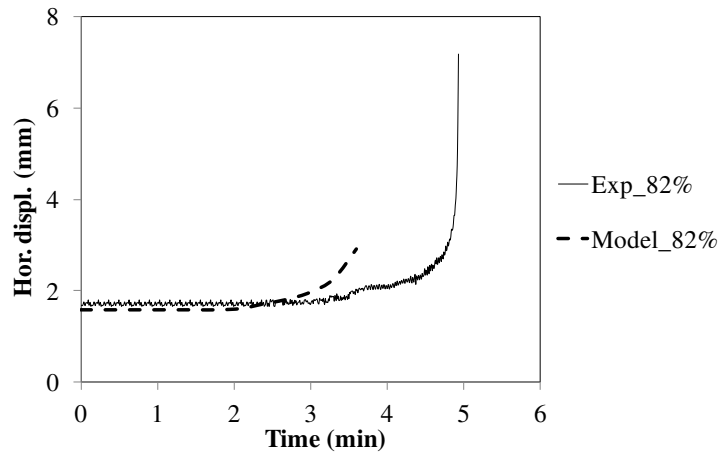
Figure 5



(a) Creep tests at 220°C – $\phi=89\%$

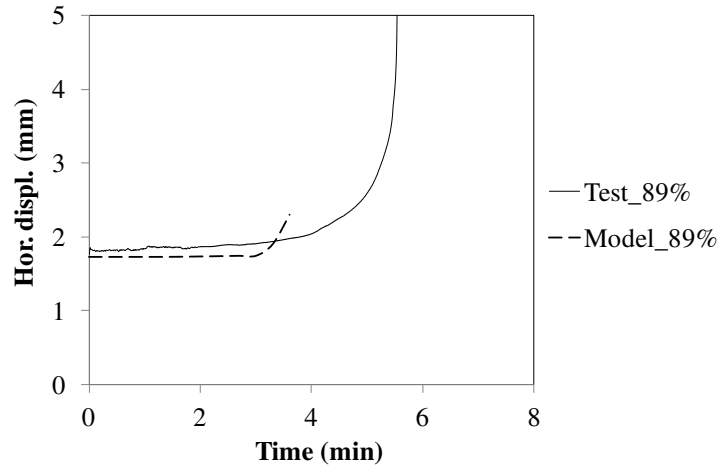


(b) Creep tests at 220°C – $\phi=84\%$

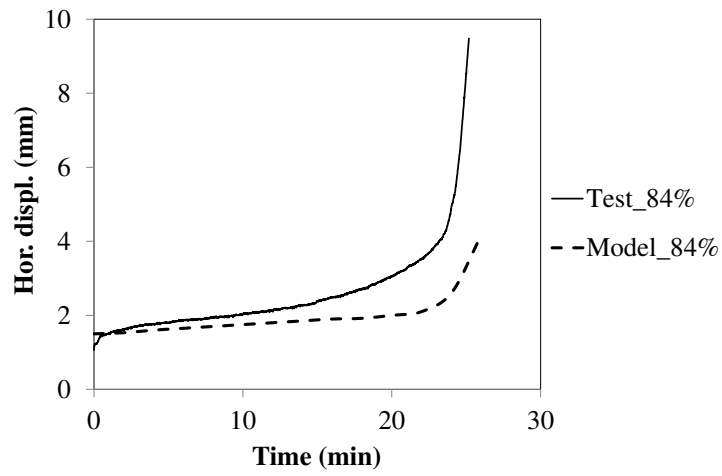


(c) Creep tests at 220°C – $\phi=82\%$

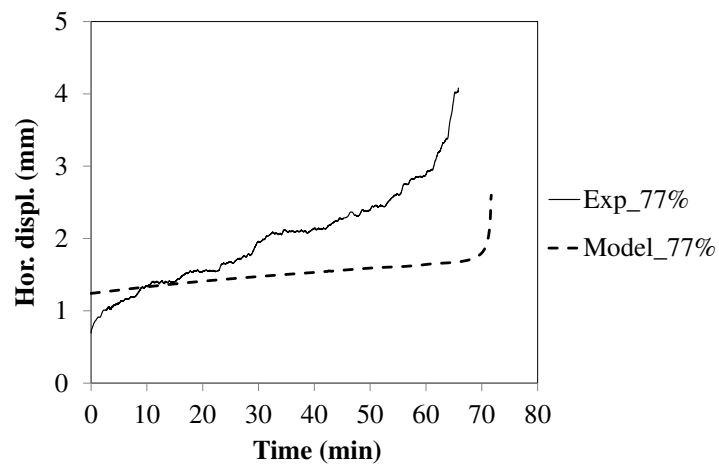
Figure 6



(a) Creep tests at 260°C – $\phi=89\%$



(b) Creep tests at 260°C – $\phi=84\%$

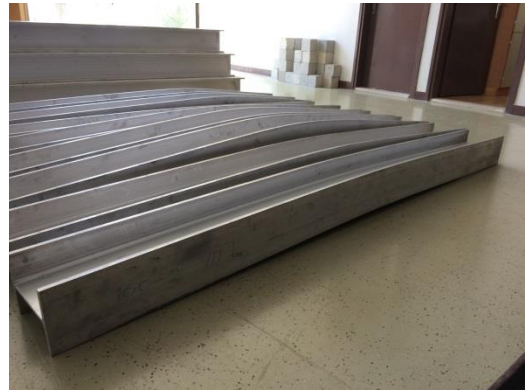


(c) Creep tests at 260°C – $\phi=77\%$

Figure 7

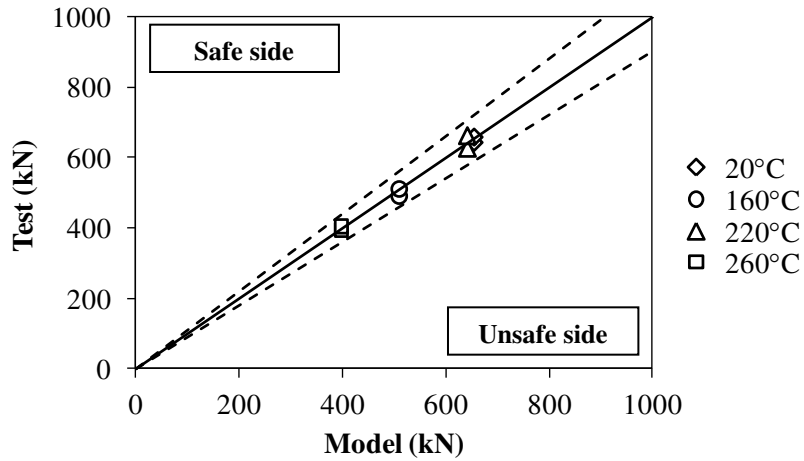


(a)

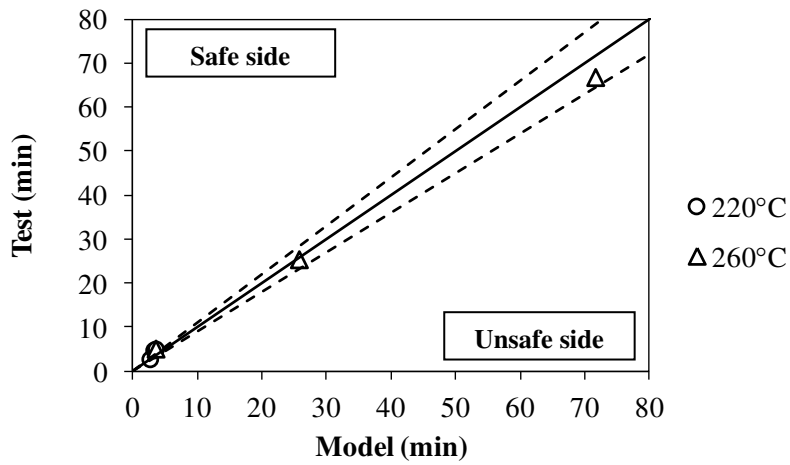


(b)

Figure 8



(a) Capacity tests: comparison with the Vulcan model.



(b) Creep tests: comparison with explicit creep modelling.

Figure 9

Table 1

Testing method		Steady-state				
Load type		Bending+Axial compression				
Target temperature (°C)		20	160	220	260	
Max. force (kN)	Test 1	Axial	640.5	488.0	624.0	392.2
		Vertical	60.0	48.1	37.7	26.0
	Test 2	Axial	656.0	508.2	659.7	402.0
		Vertical	60.0	48.1	37.7	26.0
	Average axial force (kN)		648.2	498.1	641.9	397.1

Table 2

Testing method		Steady-state			
Load type		Bending+Axial compression			
Target temperature (°C)		160	220	260	
Max. force (kN)	Test 1	Axial	427.0	524.6	305.0
		Vertical	48.0	37.7	26.0
		Load ratio ϕ (%)	86	82	77
		Failure time (min)	151.70	4.93	65.80
		Model pred. (min)	-	3.60	71.70
		Axial	457.5	536.8	332.5
	Vertical	48.0	37.7	26.0	
	Load ratio ϕ (%)	92	84	84	
	Failure time (min)	25.90	4.68	25.30	
	Model pred. (min)	-	3.30	26.30	
	Axial	475.8	573.4	353.8	
	Vertical	48.0	37.7	26.0	
	Load ratio ϕ (%)	96	89	89	
	Failure time (min)	3.60	2.66	5.53	
	Model pred. (min)	-	2.70	3.60	

Table 3

Test results / Vulcan analysis					
Temperature (°C)	20	160	220	260	
Test 1	Axial Resistance (kN)	640.5/656.0	488.0/510.0	624.0/642.0	392.2/398.0
	Spring stiffness (Nmm/rad)	1.00E+05	1.00E+05	1.00E+06	1.00E+06
Test 2	Axial Resistance (kN)	656.0/656.0	508.2/510.0	659.7/642.0	402.0/398.0
	Spring stiffness (Nmm/rad)	1.00E+05	1.00E+05	1.00E+06	1.00E+06

Table 4

Temperature (°C)	Reduction factors	
	$f_{0,\theta}/f_{0,20}$	$E_{y,\theta}/E_{y,20}$
20	1.00	1.00
100	0.97	0.99
150	0.84	0.92
200	0.66	0.92
250	0.37	0.89
300	0.20	0.68
350	0.07	0.34

Table 5

Temperature (°C)	n
20	49
100	69
150	179
200	144
250	93
300	43
350	26